analytical chemistry

Article

pubs.acs.org/ac

Gecko-Inspired Nanotentacle Surface-Enhanced Raman Spectroscopy Substrate for Sampling and Reliable Detection of Pesticide Residues in Fruits and Vegetables

Pan Wang,[§] Long Wu,[§] Zhicheng Lu, Qin Li, Wenmin Yin, Fan Ding, and Heyou Han*

State Key Laboratory of Agricultural Microbiology, College of Food Science and Technology, College of Science, Huazhong Agricultural University, Wuhan 430070, PR China

Supporting Information

ABSTRACT: Rapid sampling and multicomponent detection are crucial for monitoring of pesticide residues analysis. Here, a gecko-inspired nanotentacle surface-enhanced Raman spectroscopy (G-SERS) platform is proposed for the first time for the simultaneous detection of three kinds of pesticides via a simple and intuitive "press and peeled-off" approach. The G-SERS platform obtained from seeding deposition of silver nanoparticles (Ag NPs) on 3D PDMS nanotentacle array is flexible and free-standing. Compared with other substrates, this G-SERS substrate can simultaneously provide outstanding SERS activity (enhancement factor = 1.2×10^7), superior reproducibility (RSD = 5.8%) and countless flexible nanoscale "tentacles" ($\sim 6.7 \times 10^8/cm^2$). Moreover, the high density of "tentacles" can freely approach the microarea and enable efficient target collection, which were confirmed by SEM and HPLC. By direct sampling from cucumber, apple, and grape surfaces, thiram (TMTD), methyl parathion (MPT), malachite green (MG), and their multiple components have been rapidly and reliably determined. For example, under the optimal conditions, a sensitivity of 1.6 ng/cm^2 (S/N = 3) for TMTD was obtained on apple peels with a correlation coefficient (R) of 0.99. Therefore, the G-SERS substrate could offer a great practical potential for on-spot identification of various pesticide residues on real samples.

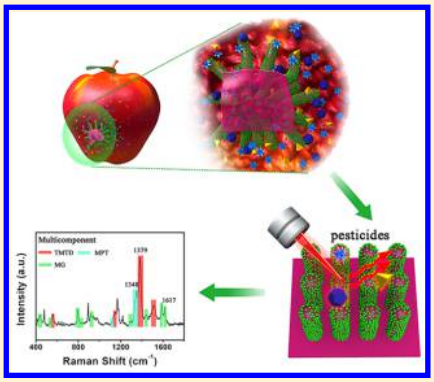

Pesticide residues in agriculture have been a crucial worldwide problem that directly threatened the environment and people's health.[1] Conventional methods for the detection of pesticide residues are always complicated, time-consuming, and require sophisticated sampling procedures, which confine their rapid application, especially the on-site analysis.[2−5] Thus, there has been a strong driving force to develop techniques such as ELISA, enzyme inhibition, and SERS for the rapid determination of pesticide residues.[6−8] Because of the advantages such as excellent sensitivity, rich molecular information, and nondestructive data acquisition, SERS has been proven to be a promising tool in public security,[9] food safety,[10] environmental monitoring,[11] and life science.[12] In the past decades, considerable efforts have been made to improve SERS signals effectively. Up until now, powerful substrates have been prepared ranging from an original rough electrode to various metal nanoparticles with prominent Raman enhancement and reproducibility,[13−17] mainly focused on addressing sensitivity and uniformity problems of the SERS substrates. However, most of those conventional substrates are based on rigid materials, such as porous alumina, silicon wafers, or glass sheet, which still encountered challenges in the rapid and microarea sampling for on-site and field-portable analysis.[18−21]

Recently, much attention has been paid to the emerging flexible substrate materials in SERS due to the excellent advantages such as low-cost, easy preparation, and ease to use.[22−26] Compared with conventional substrates, flexible materials like polymer nanofiber,[27] cellulose paper,[28] and adhesive tape[29] possess distinct capacity of intimate contact with real complex surfaces, exhibiting impressive advantages in sampling and rapid analysis with higher efficiency. Furthermore, the flexible substrates can directly collect targets from complex surfaces with negligible pretreatment through a simple approach such as "wipe", "paste and peeled-off". For example, it was reported that a SERS adhesive tap could directly collect pesticide residues from fruit and vegetable peels by a "paste and peeled-off" operation.[29] Owing to the above striking properties, flexible substrates are becoming more and more popular in on-spot SERS assay, especially in the significant on-spot trace analysis. However, limitations also exist in current flexible substrates. Some flexible substrates, such as various paper-based substrates,[31,32] do not have 3D nanostructures on their surface, which still restrict their microarea sampling efficiency on complex surface. Moreover, the unordered and discrete nanostructures on the substrates make most of the flexible substrates behave moderate sensitivity at the nanomolar level.[30,33] Motivated by these problems, we focused our work

Received: November 3, 2016
Accepted: January 16, 2017
Published: January 16, 2017

DOI: 10.1021/acs.analchem.6b04324
Anal. Chem. XXXX, XXX, XXX−XXX

on the further optimization of SERS substrates and promoted their practicability in real sample analysis.

As is well-known, gecko is a talented wall walker which originated from the large contact area produced by high density of nanoscale tentacles on their toe-pads.[34,35] Inspired by this, poly(dimethylsiloxane) (PDMS) film with gecko-like multiscale structure were constructed by the AAO template, which exhibited strong adhesive force and large contact area toward almost any surface.[36−44] Enlightened by this interesting discovery, we produced a G-SERS substrate with a surface morphology of the 3D PDMS nanotentacle array for the rapid microarea sampling and multicomponent detection of trace pesticide residues on fruits and vegetables.

Unlike the inhomogeneous nanostructure on the existing flexible substrates, in this work, highly ordered AAO was first prepared and served as reuseable templates. The prepared high density of 3D "tentacle" can freely approach microarea and make extensive contact even toward almost any surface.[39−45] As shown in Scheme 1, the PDMS nanotentacle array was first

Scheme 1. Schematic Demonstration of Preparation of G-SERS Substrate and SERS Measurement

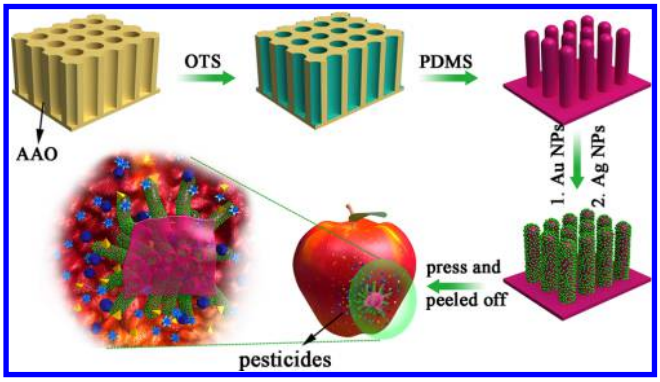

replicated from a surface-modified AAO template and then followed by O_2 plasma treatment and APTES modification. Afterward, the prepared Au NPs were absorbed on the APTES modified PDMS nanotentacle array via the electrostatic interaction and Au−N bond. Finally, the resultant Au-decorated array was soaked into freshly prepared Ag electroless deposition solution for several minutes. The prepared G-SERS substrate can enable a tremendous contact area and efficient target collection via a simple and intuitive "press and peeled-off" approach. Besides, the deposition of Ag NPs on the densely packed 3D nanotentacle array could produce considerable "hot spots" and thus ensured high enhancement of SERS signals. Hence, the G-SERS substrate is more favorable for microarea sampling and trace detection. What is more, the multi-component detection of TMTD, MPT, and MG on fruit peels are successfully achieved using the G-SERS substrate.

EXPERIMENTAL SECTION

Chemical Reagents. Methyl parathion (MPT, $C_8H_{10}NO_5PS$, 100 μg/mL in methyl alcohol), thiram (TMTD, $C_6H_{12}N_2S_4$, 97%), malachite green (MG, $C_{23}H_{25}ClN_2$, analytical grade), 4-mercaptobenzoic acid (MBA, 90%), trichlorooctadecylsilane (OTS, >85%), 3-amino-propyltriethoxysilane (APTES, 97%) were purchased from Aladdin. SYLGARD 184 Silicone Elastomer Base and SYLGARD 184 Silicone Elastomer Curing Agent were obtained from Dow Corning Corporation. Ultra pure aluminum (99.999%) was purchased from Alfa Aesar. Chloroauric acid tetrahydrate ($HAuCl_3·4H_2O$), silver nitrate ($AgNO_3$), phosphoric acid (H_3PO_4), chromium oxide (Cr_2O_3), anhydrous toluene (C_7H_8), absolute ethanol (C_2H_6O), potassium sodium tartrate ($KNaC_4H_4O_6·4H_2O$), $NH_3·H_2O$, and trisodium citrate dihydrate ($C_6H_5Na_3O_7·2H_2O$) were of analytical grade and offered by Sinopharm Chemical Reagent. All aqueous solutions were prepared with ultrapure water (resistance: 18.2 MΩ cm).

Characterizations. Raman measurements were performed using an inVia Raman spectrometer (Renishaw, U.K.) equipped with a cofocusing microscope (Leica, Germany). The SERS spectra were acquired under a He−Ne laser (633 nm) with a laser power of 10 mW with 10 s exposure and one time accumulation. SEM and TEM images were acquired with field-emission scanning microscopy (FE-SEM, SIGMA) and transmission electron microscopy (TEM, JEOL JEM-2010 microscope). The HPLC measurement was conducted on an Agilent model 1260 (Agilent Technology), equipped with a thermostat compartment for the column (250 mm, 4.6 mm, 5 μm) and diode array detector (DAD).

Fabrication of PDMS Nanotentacle Array. The PDMS nanotentacle array was prepared using a method in previous reports.[40,46,47] AAO template were fabricated by a two-step anodization of pure aluminum sheets according to previous research.[46,47] Briefly, the anodization procedure was carried out in 0.1 M phosphoric acid at 0 °C with a constant voltage of 165 V for 4 h. After the first anodization, the aluminum oxide layer was removed away using a mixture of 1.8 wt % chromic acid and 6 wt % phosphoric acid at 60 °C for 1 h, and the second anodization was conducted under identical conditions for an another 30 min. After the second anodization, the pore diameter was enlarged by a widening process in a 5 wt % phosphoric acid at 30 °C for 30 min. The surface of the template was functionalized with a self-assembled OTS monolayer to reduce surface energy between the AAO mold and PDMS,[47] then PDMS (a mixture of PDMS elastomer and curing agent) was poured onto the surface-modified AAO template and solidified in a vacuum oven at 90 °C for 1 h. After peeling the solidified PDMS from the AAO template, the PDMS nanotentacle array were obtained and the AAO template could be reused.

Preparation and Characterization of G-SERS Substrate. The PDMS nanotentacle array was treated with O_2 plasma cleaner (YZD08-5C Plasma Cleaner) at a pressure of 200 mTorr for 20 s and then immersed in 1% APTES solution in ethanol (v/v) for 15 min, followed by thoroughly washing with ethanol and drying with N_2.[36] Afterward, the APTES modified PDMS nanotentacle array were immersed in Au colloid for 2 h.[48] Finally, the resultant array was immersed in a freshly prepared Ag electroless deposition solution ($[Ag(NH_3)_2NO_3]/KNaC_4H_4O_6$ = 1:1) at room temperature for 9 min to fabricate the G-SERS substrate.[49] The G-SERS substrate was then incubated in different concentrations of 4-MBA (5 mL) for 2 h to conduct sensitivity, reproducibility, and stability analysis.

Direct Sampling and Detection of Pesticide Residues on Various Peels. Fruits and vegetables in this work are thoroughly washed with ultrapure water before use. For more reliable SERS detection, peels are cut into 1 × 1 cm^2 squares and sprayed with 10 μL of the as-prepared pesticides solution and dried at room temperature, respectively. Afterward, a drop of ethanol was sprayed onto the peels. Subsequently, the G-

DOI: 10.1021/acs.analchem.6b04324
Anal. Chem. XXXX, XXX, XXX−XXX

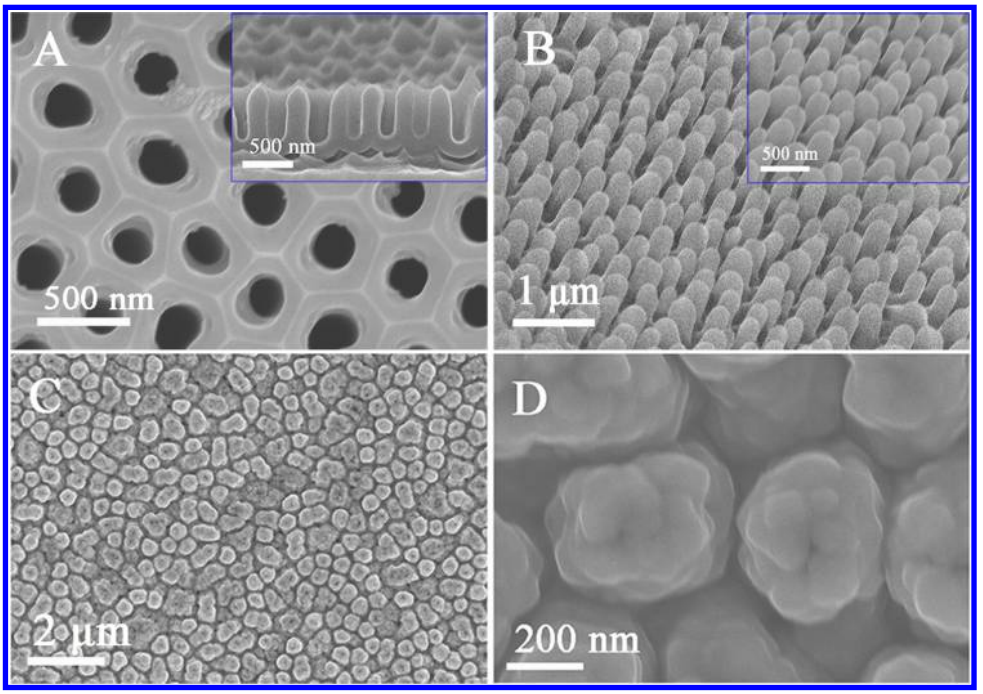

Figure 1. (A) Top-view SEM image of the AAO template (inset, side-view). (B) Tilted-view SEM image of the PDMS nanotentacle array (the inset is the amplified SEM image of part B). (C) Top-view SEM image of the G-SERS substrate with a deposition time of 9 min and (D) the amplified SEM image corresponding to part C.

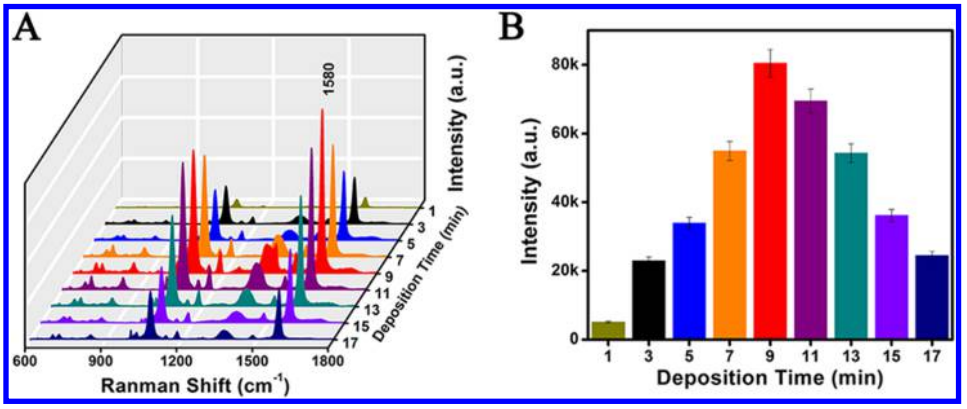

Figure 2. (A) SERS spectra of 4-MBA (10^{-5} M) molecules absorbed on corresponding G-SERS substrates. (B) Comparison of average Raman intensities at that 1580 cm^{-1} peak on the corresponding G-SERS substrates.

SERS substrate was pressed to the spiked surface and kept for a few seconds, then peeled off for further SERS analysis.

RESULTS AND DISCUSSION

Fabrication and Characterization of G-SERS Substrate. G-SERS substrate was fabricated via seeding deposition of silver nanoparticles (Ag NPs) on the 3D PDMS nanotentacle array (Scheme 1). As depicted in Figure 1A, the top-view morphology of the AAO template was orderly arranged, and the side-view further revealed the unique nanoarchitectures of the template with a depth of ~600 nm. The ordered 3D nanotentacle array was clearly observed (Figure 1B), and it can be calculated that about 6.7×10^8 nanotentacles were contained within 1 cm^2, which could provide a high density of scaffold for decorating Ag NPs in different dimensions. Owing to this flexible 3D tentacle structure, the G-SERS substrate can make extensive contact with almost any surface and enable efficient target collection.[39−44] Before the procedure of depositing silver (Scheme 1), the monodispersed Au NPs were first prepared and then covered on the nanotentacles (Figure S1). From Figure 1C,D, it can be seen that the rough Ag nanoflowers were decorated on the surface of nanotentacles and the original shape were well preserved. The 3D nanogeometries with plentiful nanogaps could offer a great deal of "hot spots" and generate large SERS enhancements under incident light.

To maximally amplify the SERS activity, a series of G-SERS substrates were prepared by applying a deposition time (DT) from 1 to 17 min at an interval of 2 min. These resultant substrates were investigated to study their SERS activity under the same conditions. Obviously, before DT reached 9 min, the SERS intensity of 4-MBA at 1580 cm^{-1} increased gradually with the increasing of DT. However, a significant SERS reduction occurred as the DT further prolonged (Figure 2A,B). All the facts have demonstrated that 9 min is the best

DOI: 10.1021/acs.analchem.6b04324
Anal. Chem. XXXX, XXX, XXX−XXX

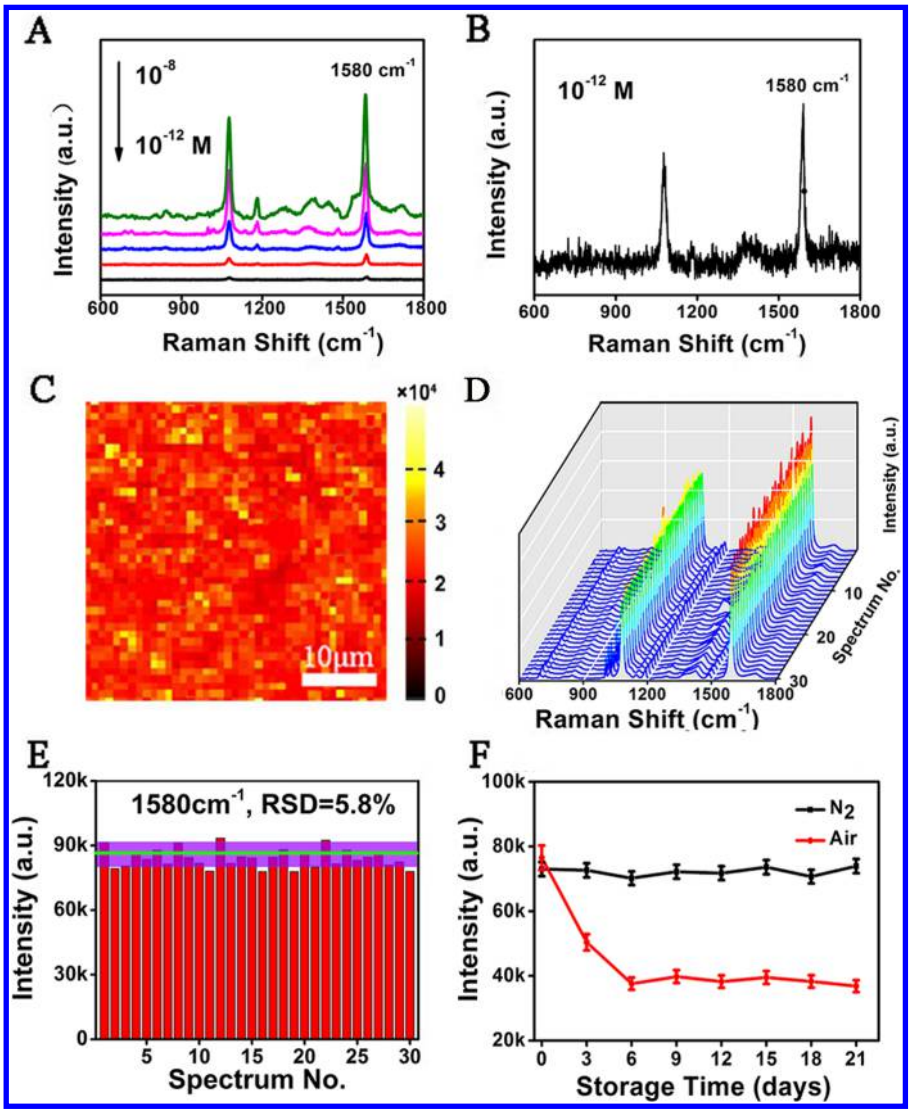

Figure 3. (A) SERS spectra of 4-MBA with the concentration ranging from 10^{-8} to 10^{-12} M using the G-SERS substrate and (B) the SERS spectra of 10^{-12} M 4-MBA. (C) SERS intensity mapping of 4-MBA (10^{-5} M) measured at the 1580 cm^{-1} peak across a 40 × 40 μm^2 piece of the G-SERS substrate. (D) SERS spectra of 4-MBA (10^{-5} M) collected at 30 sites randomly from 5 G-SERS substrates and (E) intensity distribution at 1580 cm^{-1} corresponding to part D (the average intensity is marked with green line, and the violet zones represent the ±5.8% intensity fluctuation). (F) SERS intensities of 4-MBA (10^{-5} M) enhanced by the G-SERS substrate stored in N_2 and air atmosphere at different times.

deposition time, and the corresponding substrate was chosen for further SERS analysis.

Sensitivity, Reproducibility, and Stability of G-SERS Substrate. Sensitivity, reproducibility, and stability are crucial to any SERS-active substrate. To evaluate the SERS performance of G-SERS substrate, 4-MBA was selected as a probe molecule. As illustrated in Figure 3A,B, the characteristic band of 4-MBA at 1580 cm^{-1} was used as a quantitative peak to evaluate the SERS sensitivity. It showed that 4-MBA could still be clearly identified even at a low concentration of 10^{-12} M, presenting a more splendid sensitivity than the flexible substrates reported before.[24,30] Additionally, blank control was conducted to investigate the influence of the substrate signals in the experiments (Figure S2). Nevertheless, the substrate signals were scarcely observed, indicating a weak background interference in SERS detection.

To access spot-to-spot reproducibility, SERS mapping image of G-SERS substrate was taken to demonstrate the uniformity across the entire substrate, where each pixel represented the Raman intensity of 4-MBA (1580 cm^{-1}) at the spatial position on the substrates (Figure 3C). Moreover, to further evaluate the reproducibility of substrate to substrate, the SERS signals at 30 random sites from 5 substrates were recorded and the results were depicted in Figure 3D. It was notable that all the SERS-active sites showed a relatively consistent Raman intensity. The relative standard deviation (RSD) of the Raman intensity was calculated to be about 5.8% (Figure 3E), which was better than those in similar works.[29,50,51] From these results, it can be observed that G-SERS substrate exhibited excellent sensitivity and superior reproducibility which are important to practical assays.

Also, the G-SERS substrate stability was tested under N_2 atmosphere and ambient environment storage conditions, respectively. As shown in Figure 3F, the Raman intensity decreased rapidly after it was stored for 3 days under ambient environment and still dropped down slowly until the sixth day. However, after the sixth day, the Raman intensity did not decrease further and still remained at a high level (~40 000).

DOI: 10.1021/acs.analchem.6b04324
Anal. Chem. XXXX, XXX, XXX−XXX

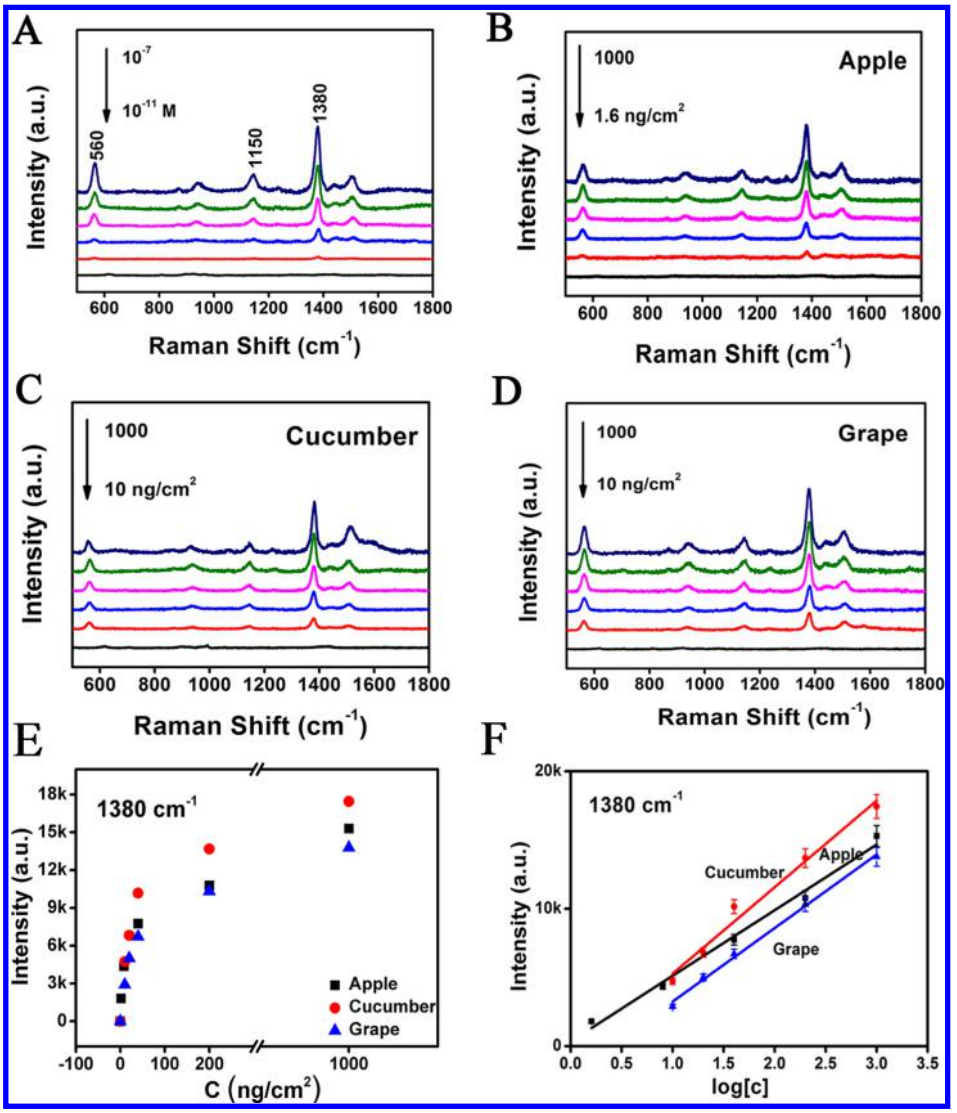

Figure 4. (A) Standard SERS spectra of TMTD enhanced by the G-SERS substrate with concentrations ranging from 10^{-7} to 10^{-11} M. (B) SERS spectra of TMTD with concentrations of 1000, 200, 40, 8, 1.6, 0 ng/cm^2 collected from the surface of apple peels, (C) concentrations of 1000, 200, 40, 20, 10, 0 ng/cm^2 collected from the surface of cucumber peels, and (D) concentrations of 1000, 200, 40, 20, 10, 0 ng/cm^2 collected from the surface of grape peels. (E) SERS intensity of TMTD from different peels (cucumber, apple, and grape) using G-SERS substrate. (F) Linear calibration plot between the SERS intensity and TMTD concentration (red, cucumber; black, apple; blue, grape).

This may be attributed to the oxide coating on the silver surface after exposing to the ambient environment, which protected Ag NPs from further oxidation and thus became stable and can be stored for longer time.[30] Though the Raman intensity decreased to a certain extent, the intensity does not have much impact on the sample detection. Moreover, G-SERS substrate exhibits convenient storage in the air without any treatment when compared to the other substrates conserved in water or other solvents.

To further demonstrate the SERS performance of the G-SERS substrate, the enhancement factor (EF), a ratio value of the enhancement of the Raman signal per molecule located on the SERS-active substrate to the normal Raman signal per molecule, was calculated according to the following formula: EF = $(I_{SERS}/N_{SERS})/(I_{NR}/N_{NR})$. Herein, I_{SERS} and I_{NR} are the intensity of the SERS and Raman signal of the same band of 4-MBA, and N_{SERS} and N_{NR} represent the corresponding number of molecules probed in the laser (633 nm) excitation area absorbed on the G-SERS substrate and in bulk solid form, respectively. In this study, the characteristic band of 4-MBA at 1580 cm^{-1} was selected for the calculation, the I_{SERS} and I_{NR} were obtained from the spectra directly, and the N_{SERS} and N_{NR} were calculated according to the previously reported work.[24] As a result, the EF is calculated to be 1.2×10^7 (the details for the EF calculation is provided in the Supporting Information), revealing an excellent enhanced performance of the G-SERS substrate.

Direct Sampling and Detection of Single Component of Pesticide on Various Fruit and Vegetable Peels. So far, it was proved that G-SERS substrate exhibited high sensitivity, superior reproducibility, and good stability. Next, the G-SERS platform was adopted to the detection of TMTD, MPT, and MG on cucumber, apple, and grape peels with a complex surface. In the spiked process, 10 μL of different concentrations of as-prepared pesticide solutions were added on the peel square and completely dried at room temperature to stimulate the natural environment. After a drop of ethanol was cast onto the spiked peel square, G-SERS substrate was pressed onto the

DOI: 10.1021/acs.analchem.6b04324
Anal. Chem. XXXX, XXX, XXX−XXX

spiked square for a few seconds and then peeled-off for further analysis (Figure S3A–D). The surface morphology of the G-SERS substrate after "press and peeled-off" operation did not show any change (Figure S3E,F), which revealed that the substrate remained the original performance and could be used for further application.

The SERS results of TMTD on cucumber, apple, and grape peels were discussed using the standard addition method. Figure 4A exhibited the SERS spectra of different concentrations of standard TMTD solutions (10^{-7} to 10^{-11} M) added to G-SERS substrate, which showed an increasing intensity as the concentration increased. Herein, the characteristic peaks of TMTD at 560 cm^{-1}, 1150 cm^{-1}, 1380 cm^{-1}, and 1508 cm^{-1} can be distinctively discerned and the peak of 1380 cm^{-1} behaved the most remarkable of the variations. Thus, we chose 1380 cm^{-1} as the standard peak to quantitatively analyze the residues on peels. Figure 4B–D presented the SERS spectra of TMTD from cucumber, apple, and grape peels collected by G-SERS substrate, respectively. The facts revealed that fluoresence noise from peels had no impact on the sample detection. Figure 4E exhibited the SERS intensity of TMTD from different peels (cucumber, apple, and grape) using G-Substrate, and Figure 4F showed the linear calibration plot between the SERS intensity and TMTD concentration. It can be concluded that the G-SERS substrate behaved a detection sensitivity of 1.6 ng/cm^2 (S/N = 3) toward TMTD on 1 cm^2 peel squares. Besides, the SERS spectra of different concentrations of MPT and MG on G-SERS substrate were exhibited in Figure S4, and the major Raman peaks of TMTD, MPT, and MG were listed in Table 1.

Table 1. Assignments and Raman Shift (cm^{-1}) for SERS Spectra of TMTD, MPT, and MG

	TMTD	
vibrational description	observed	reported[24,31]
C–N stretch, CH3 deformation	1508	15250
C–N stretch, CH3 deformation	1380	1380
C–N stretch, CH3 rock	1150	1150
SS stretch	560	580
	MPT	
vibrational description	observed	reported[24,31]
phenyl stretch	1580	1585
C–O bend	1350	1345
C–N stretch	1146	1120
P–O stretch	859	850
	MG	
vibrational description	observed	reported[26]
ring C–C stretch	1617	1620
N-phenyl stretch	1294	1300
C–H in-plane bend	1172	1170
ring C–H out-of-plane bend	915	916
ring C–H out-of-plane bend	797	798

The limit of detection (LOD) and the limit of quantity (LOQ) of TMTD, MPT, and MG residues on peels were listed in Table 2 and Table S1, which revealed that G-SERS substrate behaved acceptable performance on peels. Moreover, LOD for TMTD, MPT, and MG are much lower than those from maximum residue limits (MRL) in China and the European Union (Table S2). Thus, it can be preliminarily concluded that G-SERS substrate could be employed in pratical application.

Table 2. Analytical Results for the Quantitative SERS Detection of TMTD Residues on Cucumber, Apple, and Grape Peels

TMTD residues at different peels	*R*	LOD (ng/cm^2)	LOQ (ng/cm^2)
cucumber	0.9978	10	8.6
apple	0.9935	1.6	2.0
grape	0.9899	10	8.2

Compared with the TMTD directly added onto the substrate, the TMTD residue on peels showed much weaker Raman intensity (Figure 4A–D). Thus, it was important to explore the results caused by the incomplete sampling with "press and peeled-off" operation or the permeation of TMTD. Then HPLC was utilized to investigate the problem at a relatively high concentration of TMTD (50 ng/cm^2) on the peels. From Figure S5A, no signals of TMTD were observed in the collected washing solution, which reflected an efficient microarea sampling (the simple and intuitive "press and peeled-off" operation) of the G-SERS substrate. However, it can be seen from Figure S5B the TMTD that existed on the peels when extracting the peels in methanol. Therefore, it can be deduced that the detection difference may be caused by the permeation of TMTD into the peels.

To further access the reproducibility of this detection method in real samples, the SERS signals of TMTD at the same concentration were collected from 30 cucumbers by the "press and peeled-off" approach. As shown in Figure 5, the

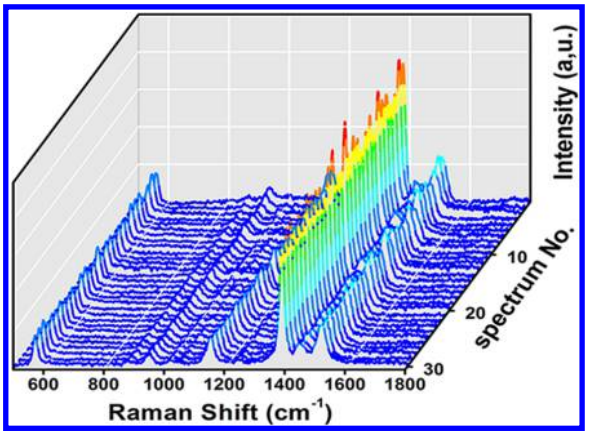

Figure 5. SERS spectra of TMTD (10 ng/cm^2) collected from 30 cucumber samples via the "press and peeled-off" approach using the G-SERS substrate.

SERS intensity of the characteristic peaks of TMTD collected from different cucumbers fluctuate in a small range. Meanwhile, the statistical results indicated a RSD (n = 30) of 9.3% with a concentration of 10 ng/cm^2 (Table 3), which revealed the high reproducibility of the proposed method in practical detection. The stability of the method on real matrixes was also explored. Typically, the G-SERS substrates were stored in ambient environment with different times and then sample TMTD

Table 3. Analytical Features of the Detection Method in Practical Analysis

concn	*R*	RSD
10 ng/cm^2	0.9978	9.3%

DOI: 10.1021/acs.analchem.6b04324
Anal. Chem. XXXX, XXX, XXX–XXX

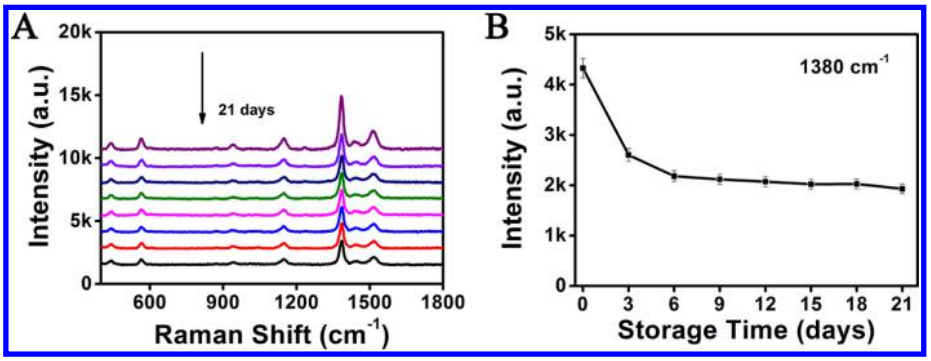

Figure 6. (A) SERS spectra of TMTD from cucumber detected by the G-SERS substrate with different storage times of 1, 3, 6, 9, 12, 15, 18, and 21 days and the corresponding SERS intensities of TMTD at 1380 cm^{-1} (B).

residue on the cucumber peels. The samples were tested under the same conditions (Figure 6). It can be seen that the SERS signals of TMTD collected from cucumber peels did not decline until it was stored more than 6 days, which revealed that the method had good stability on real matrixes.

Direct Sampling and Detection of Multiple Components of Pesticides on Various Fruit and Vegetable Peels. To protect the vegetable and fruits from diseases and insects, different pesticides such as insecticides, bactericides, and fungicides are usually blended and used, which resulted in more toxic multipesticide residues and thus created serious problems in food safety.[52] Therefore, it is encouraging to develop a method to accurately detect and quantify them. Owing to the molecularly narrow band spectra, SERS is capable of multicomponent detection without separation.[53] Thus, the proposed method was further adopted to detect the above-mentioned three pesticide mixture on cucumber. In Figure 7,

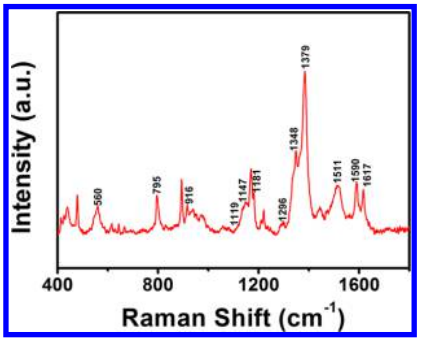

Figure 7. SERS spectra of multiple components of pesticide residues (TMTD, MG, MPT) on cucumber peels using the G-SERS substrate.

four bands at 560 cm^{-1}, 1147 cm^{-1}, 1379 cm^{-1}, and 1511 cm^{-1} are of TMTD; five bands at 795 cm^{-1}, 916 cm^{-1}, 1181 cm^{-1}, 1296 cm^{-1}, and 1617 cm^{-1} are of MG; and three bands at 1119 cm^{-1}, 1348 cm^{-1}, and 1590 cm^{-1} are of MPT. All the characteristic bands from each component can still be distinctively discerned through the spectrum. The results proved that the proposed method could be used in on-spot detection and further revealed the G-SERS substrate's powerful analytical capability in practical application. Thus, the G-SERS substrate can be employed for rapid and efficient microarea sampling of targets from complex surface and simultaneous detection of multipesticide residues in real samples, demonstrating that G-SERS substrate is a promising candidate for practical application in food safety, environmental monitoring, and life science.

CONCLUSIONS

In summary, the G-SERS platform was successfully constructed by seeding deposition of silver nanoparticles (Ag NPs) on the 3D PDMS nanotentacle array. The G-SERS substrate was utilized for the first time for rapid, efficient microarea sampling and high sensitive detection of multipesticide residues in real samples via a simple and intuitive "press and peeled-off" approach. Owing to the flexible 3D "tentacle" array, the proposed G-SERS substrate are particularly suitable for microarea sampling, *in situ* enrichment, and rapid detection of multipesticide residues. After optimization and SERS quality control tests, G-SERS substrate was successfully applied in the rapid detection of single and multicomponent pesticide residues in real samples. Compared with previous detection methods, the G-SERS substrate enabled more efficient target sampling. The excellent performance may be ascribed to the free adjustment of angle between "tentacles" and the contact surface. Moreover, the proposed method can provide unique molecular fingerprint and determine multicomponent pesticide residues in a complex system without any incubation. What is more, the low cost and convenient storage make it easy to meet the demand of practical application. In all, the proposed method has advantages related to rapid, efficient microarea sampling and simultaneous detection, which is expected to find potential applications in the food industry and the environmental field.

ASSOCIATED CONTENT

Supporting Information

The Supporting Information is available free of charge on the ACS Publications website at DOI: 10.1021/acs.analchem.6b04324.

HPLC measurements of peels and its corresponding washing solution; calculation of enhacement factor, N_{SERS}, N_{NR}; TEM image of prepared Au NPs; SERS spectra and SEM spectra of G-SERS substrate; standard SERS spectra of MG enhanced by the G-SERS substrate; HPLC results; analytical results for the quantitative SERS detection of MPT and MG residues on cucumber, apple, and grape peels; and comparison of maximum residue levels and SERS limit of detection of three pesticides on cucumber (PDF)

AUTHOR INFORMATION

Corresponding Author

*E-mail: hyhan@mail.hzau.edu.cn.

DOI: 10.1021/acs.analchem.6b04324
Anal. Chem. XXXX, XXX, XXX−XXX

ORCID

Heyou Han: 0000-0001-9406-0722

Author Contributions

[§]P.W. and L.W. had equal contribution.

Notes

The authors declare no competing financial interest.

■ ACKNOWLEDGMENTS

We gratefully acknowledge the financial support from National Natural Science Foundation of China (Grants 21375043 and 21175051) and National Key R&D Program (Grant 2016YFD0500700).

■ REFERENCES

(1) Damalas, C. A.; Eleftherohorinos, I. G. *Int. J. Environ. Res. Public Health* **2011**, *8*, 1402−1419.
(2) Zachariasova, M.; Lacina, O.; Malachova, A.; Kostelanska, M.; Poustka, J.; Godula, M.; Hajslova, J. *Anal. Chim. Acta* **2010**, *662*, 51−61.
(3) Lehotay, S. J.; Son, K. A.; Kwon, H.; Koesukwiwat, U.; Fu, W.; Mastovska, K.; Hoh, E.; Leepipatpiboon, N. *J. Chromatogr. A* **2010**, *1217*, 2548−2560.
(4) Zhao, Y.; Ma, Y.; Li, H.; Wang, L. *Anal. Chem.* **2012**, *84*, 386−395.
(5) Esteve-Turrillas, F. A.; Parra, J.; Abad-Fuentes, A.; Agullo, C.; Abad-Somovilla, A.; Mercader, J. V. *Anal. Chim. Acta* **2010**, *682*, 93−103.
(6) Fang, Q. K.; Wang, L. M.; Hua, X. D.; Wang, Y. L.; Wang, S. Y.; Cheng, Q.; Cai, J.; Liu, F. Q. *Food Chem.* **2015**, *166*, 372−379.
(7) Hou, J. Y.; Dong, J.; Zhu, H. S.; Teng, X.; Ai, S. Y.; Mang, M. L. *Biosens. Bioelectron.* **2015**, *68*, 20−26.
(8) Yang, T. X.; Zhang, Z. Y.; Zhao, B.; Hou, R. Y.; Kinchla, A.; Clark, J. M.; He, L. L. *Anal. Chem.* **2016**, *88*, 5243−5250.
(9) Jamil, A. K. M.; Izake, E. L.; Sivanesan, A.; Fredericks, P. M. *Talanta* **2015**, *134*, 732−738.
(10) Ko, J.; Lee, C.; Choo, J. *J. Hazard. Mater.* **2015**, *285*, 11−17.
(11) Fu, C.; Wang, Y.; Chen, G.; Yang, L. Y.; Xu, S. P.; Xu, W. *Anal. Chem.* **2015**, *87*, 9555−9558.
(12) Sykes, E. A.; Chen, J.; Zheng, G.; Chan, W. C. W. *ACS Nano* **2014**, *8*, 5696−5706.
(13) Camden, J. P.; Dieringer, J. A.; Zhao, J.; Van Duyne, R. P. *Acc. Chem. Res.* **2008**, *41*, 1653−1661.
(14) Banholzer, M. J.; Millstone, J. E.; Qin, L.; Mirkin, C. A. *Chem. Soc. Rev.* **2008**, *37*, 885−897.
(15) He, D.; Hu, B.; Yao, Q.-F.; Wang, K.; Yu, S.-H. *ACS Nano* **2009**, *3*, 3993−4002.
(16) Kim, K.; Han, H. S.; Choi, I.; Lee, C.; Hong, S.; Suh, S.-H.; Lee, L. P.; Kang, T. *Nat. Commun.* **2013**, *4*, 2182.
(17) Shao, F.; Lu, Z.; Liu, C.; Han, H.; Chen, K.; Li, W.; He, Q.; Peng, H.; Chen, J. *ACS Appl. Mater. Interfaces* **2014**, *6*, 6281−6289.
(18) Li, X. H.; Chen, G. Y.; Yang, L. B.; Jin, Z.; Liu, J. H. *Adv. Funct. Mater.* **2010**, *20*, 2815−2824.
(19) Ding, Q.; Liu, H.; Yang, L.; Liu, J. *J. Mater. Chem.* **2012**, *22*, 19932−19939.
(20) Liu, Y. J.; Chu, H. Y.; Zhao, Y. P. *J. Phys. Chem. C* **2010**, *114*, 8176−8183.
(21) Yu, Q.; Guan, P.; Qin, D.; Golden, G.; Wallace, P. M. *Nano Lett.* **2008**, *8*, 1923−1928.
(22) Liu, B.; Han, G.; Zhang, Z.; Liu, R.; Jiang, C.; Wang, S.; Han, M.-Y. *Anal. Chem.* **2012**, *84*, 255−261.
(23) Webb, J. A.; Aufrecht, J.; Hungerford, C.; Bardhan, R. *J. Mater. Chem. C* **2014**, *2*, 10446−10454.
(24) Shao, J.; Tong, L.; Tang, S.; Guo, Z.; Zhang, H.; Li, P.; Wang, H.; Du, C.; Yu, X.-F. *ACS Appl. Mater. Interfaces* **2015**, *7*, 5391−5399.
(25) Lee, C. H.; Tian, L.; Singamaneni, S. *ACS Appl. Mater. Interfaces* **2010**, *2*, 3429−3435.
(26) Chen, Y.; Cheng, H.; Tram, K.; Zhang, S.; Zhao, Y.; Han, L.; Chen, Z.; Huan, S. *Analyst* **2013**, *138*, 2624−2631.
(27) Severyukhina, A. N.; Parakhonskiy, B. V.; Prikhozhdenko, E. S.; Gorin, D. A.; Sukhorukov, G. B.; Moehwald, H.; Yashchenok, A. M. *ACS Appl. Mater. Interfaces* **2015**, *7*, 15466−15473.
(28) Polavarapu, L.; La Porta, A.; Novikov, S. M.; Coronado-Puchau, M.; Liz-Marzan, L. M. *Small* **2014**, *10*, 3065−3071.
(29) Chen, J.; Huang, Y.; Kannan, P.; Zhang, L.; Lin, Z.; Zhang, J.; Chen, T.; Guo, L. *Anal. Chem.* **2016**, *88*, 2149−2155.
(30) Zhu, Y.; Li, M.; Yu, D.; Yang, L. *Talanta* **2014**, *128*, 117−124.
(31) Meng, Y.; Lai, Y.; Jiang, X.; Zhao, Q.; Zhan, J. *Analyst* **2013**, *138*, 2090−2095.
(32) Yu, W. W.; White, I. M. *Analyst* **2012**, *137*, 1168−1173.
(33) Lee, C. H.; Hankus, M. E.; Tian, L.; Pellegrino, P. M.; Singamaneni, S. *Anal. Chem.* **2011**, *83*, 8953−8958.
(34) Autumn, K.; Liang, Y. A.; Hsieh, S. T.; Zesch, W.; Chan, W. P.; Kenny, T. W.; Fearing, R.; Full, R. J. *Nature (London, U. K.)* **2000**, *405*, 681−685.
(35) Autumn, K.; Sitti, M.; Liang, Y. A.; Peattie, A. M.; Hansen, W. R.; Sponberg, S.; Kenny, T. W.; Fearing, R.; Israelachvili, J. N.; Full, R. J. *Proc. Natl. Acad. Sci. U. S. A.* **2002**, *99*, 12252−12256.
(36) Lu, G.; Li, H.; Zhang, H. *Chem. Commun.* **2011**, *47*, 8560−8562.
(37) Yim, E. K. F.; Darling, E. M.; Kulangara, K.; Guilak, F.; Leong, K. W. *Biomaterials* **2010**, *31*, 1299−1306.
(38) Madaria, A. R.; Kumar, A.; Ishikawa, F. N.; Zhou, C. *Nano Res.* **2010**, *3*, 564−573.
(39) Chan, E. P.; Smith, E. J.; Hayward, R. C.; Crosby, A. J. *Adv. Mater.* **2008**, *20*, 711−716.
(40) Choi, M. K.; Yoon, H.; Lee, K.; Shin, K. *Langmuir* **2011**, *27*, 2132−2137.
(41) Lin, P.-C.; Vajpayee, S.; Jagota, A.; Hui, C.-Y.; Yang, S. *Soft Matter* **2008**, *4*, 1830−1835.
(42) Lee, D. Y.; Lee, D. H.; Lee, S. G.; Cho, K. *Soft Matter* **2012**, *8*, 4905−4910.
(43) Rahmawan, Y.; Chen, C.-M.; Yang, S. *Soft Matter* **2014**, *10*, 5028−5039.
(44) Xi, J.; Jiang, L. *Ind. Eng. Chem. Res.* **2008**, *47*, 6354−6357.
(45) Isla, P. Y.; Kroner, E. *Adv. Funct. Mater.* **2015**, *25*, 2444−2450.
(46) Lee, S. G.; Lee, D. Y.; Lim, H. S.; Lee, D. H.; Lee, S.; Cho, K. *Adv. Mater.* **2010**, *22*, 5013−5017.
(47) Lee, D. Y.; Lee, D. H.; Lim, H. S.; Han, J. T.; Cho, K. *Langmuir* **2010**, *26*, 3252−3256.
(48) Jana, N. R.; Gearheart, L.; Murphy, C. J. *Langmuir* **2001**, *17*, 6782−6786.
(49) Lu, L. H.; Eychmuller, A.; Kobayashi, A.; Hirano, Y.; Yoshida, K.; Kikkawa, Y.; Tawa, K.; Ozaki, Y. *Langmuir* **2006**, *22*, 2605−2609.
(50) Gong, Z.; Du, H.; Cheng, F.; Wang, C.; Wang, C.; Fan, M. *ACS Appl. Mater. Interfaces* **2014**, *6*, 21931−21937.
(51) Oh, Y.-J.; Jeong, K.-H. *Adv. Mater.* **2012**, *24*, 2234−2237.
(52) Zhang, Y.; Wang, Z.; Wu, L.; Pei, Y.; Chen, P.; Cui, Y. *Analyst* **2014**, *139*, 5148−5154.
(53) Fang, W.; Zhang, X.; Chen, Y.; Wan, L.; Huang, W.; Shen, A.; Hu, J. *Anal. Chem.* **2015**, *87*, 9217−9224.

DOI: 10.1021/acs.analchem.6b04324
Anal. Chem. XXXX, XXX, XXX−XXX